Proceedings of the ASME 2021
International Mechanical Engineering Congress and Exposition
IMECE2021
August 17-20, 2021, Online Conference

IMECE2021-71078

DYNAMIC SIMULATION OF REEVING SYSTEMS WITH THE EXTENSION OF THE MODAL APPROACH IN THE AXIAL DIRECTION

Narges Mohammadi, José Luis Escalona*

Department of Mechanical and Material Engineering, University of Seville, Seville, Spain

ABSTRACT

In this work, the simulation of reeving systems has been studied by including axial modes using the Arbitrary Lagrangian-Eulerian (ALE) description. The reeving system is considered as a deformable multibody system in which the rigid bodies are connected by the elastic wire ropes through sheaves and reels. A set of absolute nodal coordinates and modal coordinates is employed to describe the motion and deformation in the axial direction. This new method allows the analysis of elements with non-constant axial strain along its length. In addition, modal coordinates are employed to describe the dynamic motion in the transverse direction. The non-constant axial displacement within the wire rope is computed in terms of the absolute position coordinates, longitudinal material coordinates, and modal deformation coordinates. To derive the governing equations of motion, Lagrange's equation is employed. The formulation is validated for a simple pendulum-like motion actuated by an initial velocity. The simulation results are provided to trace the movements of the payload. It can be seen that by adding modal coordinates, the axial force within the element changes. Moreover, the effects of modal coordinates in the axial direction are presented for a different number of nodes, and the resulting axial forces are compared with reference solution.

Keywords: Arbitrary Lagrangian-Eulerian description, Reeving Systems, Wire-rope elements, Flexible multibody dynamics, Transverse oscillations, Modal approach

1. INTRODUCTION

Reeving systems can be defined as large-deformable multibody systems in which rigid bodies and wire ropes are connected using sheaves and reels. These systems are usually actuated by a motor acting on a drive sheave, where the power of the motor to the payload is transmitted using wire ropes and deviation sheaves. This mechanism is able to transport a large amount of motion and large power in a long distance with a small space. Some examples of the application of these systems in real-world life can be seen in cranes, elevators, ropeways, and other hoisting devices. In most of these applications, the accuracy in the positioning or a safe ride plays an important role. Therefore, it is essential to correctly address these mechanisms and their different elements [1, 2].

Ropes and cables are the most important elements of reeving systems. Large deformation of these elements is the reason that studying their dynamic behavior is a challenging task. Moreover, there are important factors affecting the behavior of wire ropes in a reeving system, such as transverse vibrations in spans and their interaction with sheaves or pulleys, which all require to be identified correctly. Many models have been proposed to address these slender elements. For example, wire ropes can be model as Cosserat, extensible Kirchhoff, or inextensible Kirchhoff models. Of these different models, the extensible Kirchhoff model can be an appropriate choice to describe the behavior of wire ropes in reeving systems. This model can describe axial and torsion deformations. However, shear deformation is not possible to be addressed using this model. This deformation does not significantly affect the overall dynamics of reeving mechanisms because of the large sheave radius compared to the thickness of the wire rope. Moreover, the shear deformation of wire ropes is complicated to model because the cross-section is a set of independent sections of the wires. Nevertheless, some studies have modeled the shear effects in belt pulley systems [3, 4].

There are different discretization methods used for wire-rope elements. One of the most straightforward models considers wire ropes as elastic linear springs with length-dependent stiffness in which the wire-rope weight and inertia forces are neglected. Although this model cannot address lateral vibration, it can be employed in many industrial applications [5]. There are also other models, such as a lumped-parameters discretization (spring-mass model) [6] and the Rayleigh-Ritz method [7]. These models can successfully address the rope inertia forces and lateral vibrations in non-steady conditions. A recently-developed discretization method to describe cables and belts is the Absolute Nodal Coordinate Formulation (ANCF). This method has been employed to address the dynamic behavior of

cables in a three-dimensional pantograph/catenary system. The results of this study demonstrate the high accuracy of this method [8]. This method has many advantages, in particular, for beam structures [9]. In the case of varying-length wire ropes, this method can also present a realistic model, but it requires a large number of elements. In other words, it uses the same fine mesh size all along the ropes. To overcome this problem, the Eulerian-Lagrangian method can be a proper alternative. This method can successfully be employed to describe small deformations in the wire rope with a large variation of the length of spans [2,3].

The Lagrangian formulation can be used for problems with small deformation as in solid mechanics, whereas the Eulerian formulation can be employed for problems with large deformation as in fluid mechanics. Therefore, for problems involving a combination of these two types of deformation, the Arbitrary Lagrangian-Eulerian (ALE) formulation, a combination of these methods can be utilized. This method allows nodes to move freely within the described body to model the problem. In other words, the reference domain is not tied in the global frame or material coordinates. Hence, the nodal points can be represented in terms of time-dependent material coordinates and geometric coordinates, which change within the flexible body. Moreover, a fine mesh can only be employed for the contact region, and a coarse mesh is used for non-contact areas. Therefore, the computational efficiency of the problem can significantly be enhanced by reducing the total number of degrees of freedom (DOF). It should be mentioned that using such a formulation also complicates the governing dynamic equations. Some applications of this method include metal-manufacturing, the simulation of mass-variable systems, and fluid-structure interaction problems. One of the first studies on using the ALE method in reeving systems is presented for modeling of sliding joints [1, 10-11]. Some studies have employed the ALE method for addressing the dynamical behavior of reeving systems. For example, the transverse vibrations of the flexible multibody reeving systems have been studied using the ALE method. In this study, Lagrange equations have been employed to investigate the axial and transverse vibrations. The resulting deferential-algebraic equations have been solved using the Lagrange multipliers method and coordinate partitioning method [3]. The same approach has been applied for reeving systems by including axial-torsion elastic coupling [1].

In addition, there are other studies on the overall behavior of reeving systems using different approach. For example, the coupled lateral–longitudinal motion of a deep mine hoisting cable system is simulated using the moving coordinate frame approach. In this research, Hamilton's principle is employed to derive the nonlinear partial differential equations, which arise from the interaction between lateral and longitudinal vibrations. Using the Rayleigh-Ritz method, the resulting equations have been reduced to a coupled system of nonlinear second-order differential equations [12]. Moreover, the dynamic behavior of the cable-pulley systems during winding has been addressed by considering the contact between cable and pulley. The dynamic equations of this study are obtained based on the principle of virtual power and by accounting for the tensile strain, gravity, and inertial forces on the cable. To discretize the cable, the finite element method with Lagrangian cubic elements has been adopted. Finally, using the reduction technique of degrees of freedoms, the results are presented for different lifting mechanisms [13]. Recently, the transverse vibration of a high-speed elevator system has been conducted based on the continuum mechanics approach and Hamilton principle. In this study, the Galerkin method has been employed to discretize the problem. The results of this study have been presented for cases with and without damping, and the effect of damping in reducing the vibration has been demonstrated [14]. In another study, the vibrational behavior of a reeving system with a compensating rope has been investigated using a modal approach. The governing equations have been obtained by employing Hamilton's principle in longitudinal and transverse directions, and discretized using Green's formula. Finally, to solve the resulting differential-algebraic equations, the generalized-α method has been used [15].

The results so far have only considered the modal coordinate approach for the lateral deformation; therefore, only constant tension can be described in the axial direction. However, in this study, modal coordinates have also been employed for axial deformations. To derive the governing equations, firstly, the kinematic relationships of wire ropes as slender structures are described. Using the ALE method, the deformation of the wire element in the axial direction is described using absolute nodal coordinate and modal coordinates. Moreover, the lateral deformations are described using modal coordinates. In the next part, the equations of motion of reeving systems are obtained as the multibody systems. Using Lagrange equations, the equations of motion of rigid bodies and wire ropes are obtained in a matrix form. To solve the resulting equations, the coordinate portioning method together with the Runge-Kutta method are employed. Moreover, in this study, owing to the complexity of the elastic force terms, the analytical method is not any more efficient to obtain the generalized elastic forces. Hence, the Gauss quadrature method has been employed to obtain the elastic forces. Finally, the resulting simulation is validated with the previous study and the effects of axial modes are described.

2. Mathematical Formulations

2.1 Kinematic description

To analyze the dynamic behavior of a reeving system using the ALE method, a hybrid set of coordinates is considered as follows.

$$\mathbf{q} = \begin{bmatrix} \mathbf{q}_a^T & \mathbf{q}_m^T & \mathbf{q}_s^T \end{bmatrix}^T \tag{1}$$

where $\mathbf{q}_a$ is the absolute position vector coordinates of the nodal points with respect to the fixed global reference frame at the two endpoints of ALE-FEM element as:

$$\mathbf{q}_a = \begin{bmatrix} \mathbf{r}_1^T & \mathbf{r}_2^T \end{bmatrix}^T \tag{2}$$

Moreover, $\mathbf{q}_s = [s_1 \quad s_2]^T$ is the time-dependent longitudinal coordinates of the nodal points with respect to the reference-straight configuration of the body frame. The vector $\mathbf{q}_m$ also includes the modal coordinates in the transverse and axial directions as:

$$\mathbf{q}_m = [q_{x1} \quad \cdots \quad q_{xn} \quad q_{y1} \quad \cdots \quad q_{yn} \quad q_{z1} \quad \cdots \quad q_{zn}]^T \tag{3}$$

Using the defined set of coordinates, the absolute position vector, $\mathbf{r}$, of a point within the ALE element can be stated as a sum of the absolute position vector, $\mathbf{r}_a$, and the displacement, $\mathbf{u}_t$, as:

$$\mathbf{r} = \mathbf{r}_a + \mathbf{u}_t = \mathbf{N}(s, \mathbf{q}_s)\mathbf{q}_a + \mathbf{A}_e(\mathbf{q}_a)\bar{\mathbf{u}}_t \tag{4}$$

where $\mathbf{A}_e$ is the rotation matrix associated with the segment-fixed frame that can be stated in terms of the unit vectors as:

$$\mathbf{A}_e(\mathbf{q}_a) = [\mathbf{i}_e \ \mathbf{j}_e \ \mathbf{k}_e] \tag{5}$$

in which $\mathbf{i}_e$ for a segment-fixed frame can be defined by defining a unit length vector in the longitudinal direction of an element using the absolute positions of nodal points 1 and 2. This unit vector forms the first column for the rotation matrix. The remaining two columns, that is, $\mathbf{j}_e$ and $\mathbf{k}_e$, can be obtained using an orthogonalization method.

Moreover, $\mathbf{N}(s, \mathbf{q}_s)$ is the shape function matrix that can be written in terms of the longitudinal coordinates. In this problem, shape functions are considered to be linear, which are sufficient for the axial analysis.

$$\mathbf{N}(s, \mathbf{q}_s) = [N_1(s)\mathbf{I}_{3\times3} \quad N_2(s)\mathbf{I}_{3\times3}] \tag{6}$$

$$N_1(s) = \frac{1-\xi(s)}{2}, \ N_2(s) = \frac{1+\xi(s)}{2} \tag{7}$$

$$\xi(s) = \frac{2s - s_1 - s_2}{s_2 - s_1}. \tag{8}$$

Finally, vector $\mathbf{u}_t$ in the Equation (4), includes the components of the elastic displacements with respect to the segment-fixed frame. This vector can be computed as:

$$\bar{\mathbf{u}}_t = \mathbf{S}(s, \mathbf{q}_s)\mathbf{q}_m \tag{9}$$

where $\mathbf{S}$ is the shape function matrix corresponding to the transverse and axial deformations of the element. In a general format, it can be stated as:

$$\mathbf{S}(s, \mathbf{q}_s) = \begin{bmatrix} S_1 & \cdots & S_n & 0 & \cdots & 0 \\ 0 & \cdots & 0 & S_1 & \cdots & S_n \\ 0 & \cdots & 0 & 0 & \cdots & 0 \\ 0 & \cdots & 0 & & & \\ 0 & \cdots & 0 & & & \\ S_1 & \cdots & S_n & & & \end{bmatrix} \tag{10}$$

$$S_i(s) = \sin\frac{i\pi(s - s_1)}{s_2 - s_1}, \ i = 1, \ldots, n. \tag{11}$$

The velocity of nodal points can also be obtained as the time derivative of the position vector as below:

$$\dot{\mathbf{r}} = \dot{\mathbf{r}}_a + \dot{\mathbf{u}}_t = \dot{\mathbf{N}}\mathbf{q}_a + \mathbf{N}\dot{\mathbf{q}}_a + \dot{\mathbf{A}}_e\mathbf{S}\mathbf{q}_m + \mathbf{A}_e\dot{\mathbf{S}}\mathbf{q}_m + \mathbf{A}_e\mathbf{S}\dot{\mathbf{q}}_m \tag{12}$$

The above equation can be expressed in a simplified form by neglecting some terms that have a trivial effect on the final value of velocity. As in the reeving systems, the transverse velocity of the points in the wire cables is large compared to the length variation of the cable spans between sheaves; it is acceptable to neglect the third and fourth elements of the velocity equation, Equation (12). Therefore, the velocity formulation can be simplified and rewritten in a matrix form as:

$$\dot{\mathbf{r}} \approx \dot{\mathbf{N}}\mathbf{q}_a + [\mathbf{N} \quad \mathbf{A}_e\mathbf{S}]\begin{bmatrix} \dot{\mathbf{q}}_a \\ \dot{\mathbf{q}}_m \end{bmatrix} \tag{13}$$

2.1 Dynamic description

To obtain the equation of motion of an element, the Lagrange equation has been employed as:

$$\frac{d}{dt}\frac{\partial T}{\partial \dot{\mathbf{q}}} - \frac{\partial (T - U)}{\partial \mathbf{q}} = \mathbf{Q} \tag{14}$$

where U is the deformation energy, T is the kinetic energy of the ALE-FEM element that can be expressed in terms of the velocity of the nodal points as:

$$T = \frac{1}{2}\int_{s_1}^{s_2} \rho A \dot{\mathbf{r}}^T \dot{\mathbf{r}} ds \tag{15}$$

The right-hand side of the Equation (14), including the kinetic energy term, is called the generalized inertia forces that can be written in terms of quadratic-velocity inertia force $\mathbf{Q}_\mathbf{v}$ and the mass matrix $\mathbf{M}$ as:

$$\frac{d}{dt}\frac{\partial T}{\partial \dot{\mathbf{q}}} - \frac{\partial (T)}{\partial \mathbf{q}} = \mathbf{M}\ddot{\mathbf{q}} + \mathbf{Q}_\mathbf{v} \tag{16}$$

$$\mathbf{Q}_\mathbf{v} = -\frac{\partial}{\partial \mathbf{q}}\left(\frac{\partial T}{\partial \dot{\mathbf{q}}}\dot{\mathbf{q}}\right) + \frac{\partial T}{\partial \mathbf{q}} \tag{17}$$

$$\mathbf{M} = \frac{\partial}{\partial \dot{\mathbf{q}}}\left(\frac{\partial T}{\partial \dot{\mathbf{q}}}\right) \tag{18}$$

A model that accounts for axial deformation as well as transverse vibration, the deformation energy can be presented as:

$$U_{elas} = \frac{1}{2}\int_{s_1}^{s_2} EA\varepsilon^2 ds + \frac{1}{2}\int_{s_1}^{s_2} EI\kappa^2 ds + \frac{1}{2}\int_{s_1}^{s_2} P\left(\frac{\partial u_t}{\partial s}\right)^2 ds \tag{19}$$

in which three integrals comprise terms that account for deformation energy in the longitudinal direction (U_{ax}), transverse bending (U_{bend}), and additional term, namely, taut-string deformation energy (U_{str}), which is a result of axial load to transverse displacement coupling. The longitudinal

deformation, ε, and the curvature, κ, in Equation (12) can be computed as:

$$\varepsilon = \frac{1}{2}\left(\left(\frac{\partial \mathbf{r}}{\partial s}\right)^T\left(\frac{\partial \mathbf{r}}{\partial s}\right)-1\right),\ \kappa = \left\|\frac{\partial^2 \mathbf{r}}{\partial s^2}\right\|. \tag{20}$$

In addition, the axial load P on the segment can be obtained in terms of the tensile force vector, $\mathbf{F}_{ax}$, as:

$$P = \|\mathbf{F}_{ax}\|, \quad \text{and} \quad \mathbf{F}_{ax} = EA\varepsilon \tag{21}$$

By taking the partial derivative of the deformation energy per Equation (19), the generalized elastic forces can be obtained as:

$$\mathbf{Q_{elas}} = -\frac{\partial U_{elas}}{\partial \mathbf{q}} \tag{22}$$

Finally, the last term in Equation (14), $\mathbf{Q}$, is the generalized external forces, including the generalized reaction forces $\mathbf{Q_{reac}}$ due to the kinematic constraints, and the generalized applied forces $\mathbf{Q_{ext}}$. Generalized applied forces can be expressed as a function of the generalized coordinates, generalized velocities, and time. Some examples of generalized applied forces can be gravity forces, spring-dashpots forces, aerodynamic forces, etc. Therefore, by substituting all force terms in the Lagrange equation, the final governing equation of the element can be stated as:

$$\mathbf{M\ddot{q}} = \mathbf{Q_v} + \mathbf{Q_{elas}} + \mathbf{Q_{ext}} + \mathbf{Q_{app}} + \mathbf{Q_{reac}} \tag{23}$$

By assembling the equations of motions of rigid bodies and wire ropes, the system of governing equations for a system with ne wire ropes can be written in a matrix form as:

$$\begin{bmatrix} \mathbf{M}^{rb} & 0 & \dots & 0 \\ 0 & \mathbf{M}^{wr_1} & \dots & 0 \\ \vdots & \vdots & \ddots & \vdots \\ 0 & 0 & \dots & \mathbf{M}^{wr_{ne}} \end{bmatrix} \begin{bmatrix} \ddot{q}^{rb} \\ \ddot{q}^{wr_1} \\ \vdots \\ \ddot{q}^{wr_{ne}} \end{bmatrix} = \tag{24}$$

$$\begin{bmatrix} \mathrm{Q}^{rb} \\ \mathrm{Q}^{wr_1} \\ \vdots \\ \mathrm{Q}^{wr_{ne}} \end{bmatrix} + \begin{bmatrix} \mathrm{Q}^{rb}_{reac} \\ \mathrm{Q}^{wr_1}_{reac} \\ \vdots \\ \mathrm{Q}^{wr_{ne}}_{reac} \end{bmatrix}$$

where superscript rb and wr_i, with $i = 1,2,...,ne$ stand for the rigid body and wire ropes, respectively. Moreover, $\mathbf{Q}_{wr_i}$ is the generalized force vector, including applied forces, elastic forces and quadratic-velocity forces. Regarding generalized reaction forces, using the method of the Lagrange multipliers for holonomic constraints, they can be calculated in terms of the Jacobian of the constraint equations with respect to the generalized coordinates as:

$$\mathbf{Q^h_{reac}} = -\mathbf{C_q}\lambda^h \tag{25}$$

Substituting Equation (25) into the Equation (24), the final set of equations that include n scalar equations and $n + m_h$ unknowns are obtained. To find all unknowns, the final equations should be augmented with the second derivative of the nonlinear constraints, Equation (25). Finally, the resulting system of differential-algebraic equations (DAE) can be stated in a compact form as:

$$\begin{bmatrix} \mathbf{M} & \mathbf{C_q}^T \\ \mathbf{C_q} & 0 \end{bmatrix} \begin{bmatrix} \ddot{\mathbf{q}} \\ \lambda \end{bmatrix} = \begin{bmatrix} \mathbf{Q} \\ -\dot{\mathbf{C}}_\mathbf{q}\dot{\mathbf{q}} - \mathbf{C}_t \end{bmatrix} \tag{26}$$

Both mass matrix and the generalized forces have been computed using the symbolic calculation in the MATLAB environment. All the terms in Equation (26), have been computed analytically. However, due to the complexity of the generalized elastic force term, the numerical integration with the Gaussian quadrature of U_{elas} has been employed to compute it. To solve the resulting formulation, the coordinate partitioning method (dependent and independent coordinates are chosen manually) has been used. Moreover, the explicit Runge-Kutta method has been selected to solve the final dynamic equations.

3. Numerical examples

To demonstrate the effect of axial modes in evaluating transverse and axial deformation, a simple pendulum-like motion has been considered. The schematic of the system is depicted in Figure 1. Moreover, the simulation parameters are tabulated in Table 1. The only external excitation is the horizontal velocity that is applied at the initial instant to the load or rigid body. There is no other excitation, such as a motor torque, and both sheaves are fixed in space.

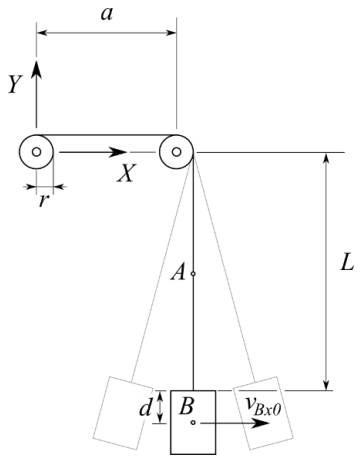

FIGURE 1: PENDULUM-LIKE MOTION OF THE TWO-BRANCH WIRE-ROPE SYSTEM

To describe the dynamic behavior of the system, the total set of coordinates of the reeving system is divided into two subsets, including rigid body coordinates $\mathbf{q}_{rb}$ and wire rope coordinates $\mathbf{q}_{wr}$. The given system in Figure 1 only includes 1 rigid body, which is the payload. The coordination used to describe the movement of this payload in the 3D space is as:

$$\mathbf{q}_{rb} = \begin{bmatrix} r_x^B & r_y^B & r_z^B & \theta_0^B & \theta_1^B & \theta_2^B & \theta_3^B \end{bmatrix} \quad (27)$$

in which r_x^B, r_y^B, and r_z^B represent the absolute positions of the payload in the x, y, and z directions, respectively. Additionally, θ_i^B, $i = 0, 1, 2, \text{and } 3$ are quaternion representations of the rotation that must fulfill the following nonlinear constraint.

$$(\theta_0^B)^2 + (\theta_1^B)^2 + (\theta_2^B)^2 + (\theta_3^B)^2 - 1 = 0 \quad (28)$$

Table 1: GEOMETRIC AND MECHANICAL PARAMETERS OF THE REEVING SYTSEM

Parameter	Value	Units	Description
a	3	m	Distance between pulleys
L	20	m	Length of the vertical rope span in the undeformed configuration
d	0.3	m	Distance between rope attachment point and payload center of mass
r	0.1	m	Radius of the pulleys
g	9.81	m/s2	Gravitational acceleration
ρA	0.6205	kg/m	Mass per unit length
EA	16.5	MN	Axial stiffness
EI	30.9	N m2	Bending stiffness
MB	1000	kg	Mass of the payload
JB	36	Kg m2	Moment of inertia of load B

The wire-rope coordinates, $\mathbf{q}_{wr}$, includes $\mathbf{q}^a$, and $\mathbf{q}^b$. As mentioned earlier, each set of nodal coordinate includes 17 coordinates, including 6 components for the absolute position vectors at endpoints, 9 coordinates for axial modal coordinate and the transverse modal coordinates in two directions, and the 2 last elements for the arc-length coordinates of the nodal points. The total set of nodal coordinates in this example is:

$$\mathbf{q}_{wr} = \begin{bmatrix} \mathbf{q}^{aT} & \mathbf{q}^{bT} \end{bmatrix}^T \quad (29)$$

Therefore, the total number of coordinates required to model the behavior of the given system is equal to $17 \times 2 + 7 = 41$. However, this system is subjected to the linear and nonlinear constraints that decrease the number of degrees of freedom.

According to the given assumptions of the reeving system in the previous part, the linear constraints imposed on the system can be stated:

$$\begin{aligned} & r_z^{a1} = 0,\ \mathrm{r}_z^{a2} = a,\ \mathrm{r}_z^{b1} = r_z^{a2},\ \mathrm{r}_z^{b2} = l \\ & s_1^a = 0,\ s_1^b = s_2^a,\ s_2^b = l + a \end{aligned} \quad (30)$$

In addition, for the modes in transverse directions, only one mode in each direction has been considered.

Regarding modal coordinates in axial direction, three possible cases have been considered, which are one, two, and three axial modes for each wire rope. Therefore, according to these different assumptions, the number of degrees of freedom can change. On the other hand, due to the geometry of the problem, all coordinate values in the z direction are set to be zero as:

$$z_1^i = z_2^i = 0 \quad (31)$$

Regarding the nonlinear constraints, there is only one constraint for the wire rope, which is the equivalence of the axial loads at the deviation sheaves as:

$$F_a^{ax} - F_b^{by} = 0. \quad (32)$$

Additionally, as stated before, the rigid body also undergoes one nonlinear constraint, which is related to the quaternion parameters, Equation (28). The nonlinear constraints can be employed to obtain the dependent coordinates in terms of the independent coordinates, which are the degrees of the freedom of the system. Obtaining all values of independent and dependent coordinates at each time instant, all other coordinates can easily be obtained using linear constraints.

4. RESULTS AND DISCUSSION

In this part, the simulation results are presented for the simple pendulum-like motion of the previous section. Firstly, to validate the accuracy of the formulations and numerical integration, the numerical integration results are compared with the reference solutions in Figure 2. In the reference solution, no axial mode is considered in the formulation, and generalized elastic forces are integrated symbolically. However, in the numerical method, the different number of modes (one, two, and three) have been considered; and generalized elastic forces are computed numerically using the Gaussian quadrature. As can be seen, the numerical results with one and three modes agree well with the analytical method.

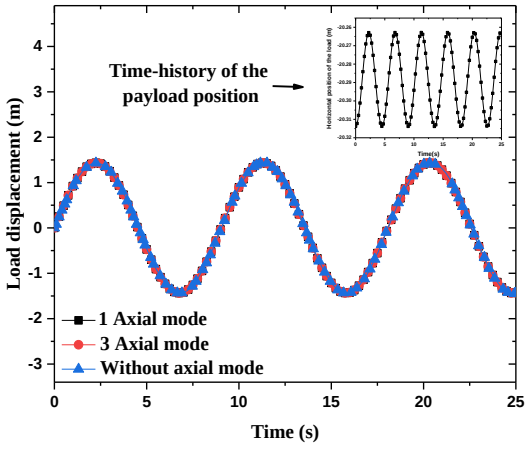

FIGURE 2: LOAD DISPLACEMENT IN HORIZONTAL DIRECTION FOR THREE CASES: ANALYTHICAL METHOD WITHOUT AXIAL LOAD, NUMERICAL METHOD WITH INCLUDING ONE AND THREE AXIAL MODES.

Moreover, Figure 3 shows the variation of the axial force versus time for different numbers of modes along the wire rope

(b). It can be observed that the variation of the axial load within the wire rope is changing by adding more modes. However, at the end of the wire rope, the values of axial force are very close to each other for these three cases. In the Figure 4, the time history of the axial force at the end of the wire rope for different cases is compared.

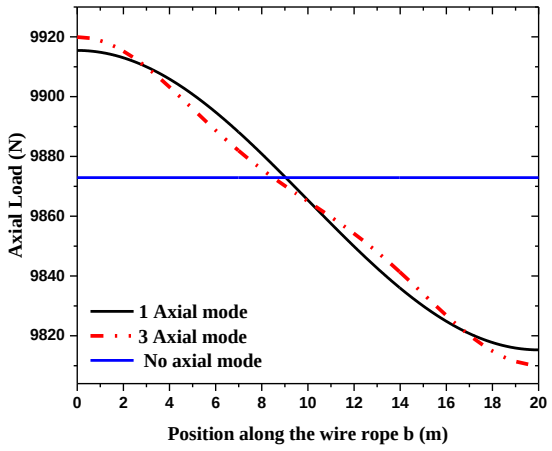

FIGURE 3: THE VARIATION OF THE AXIAL LOAD ALONG THE WIRE ROPE AT STATIC EQUILIBRIUM POSITION

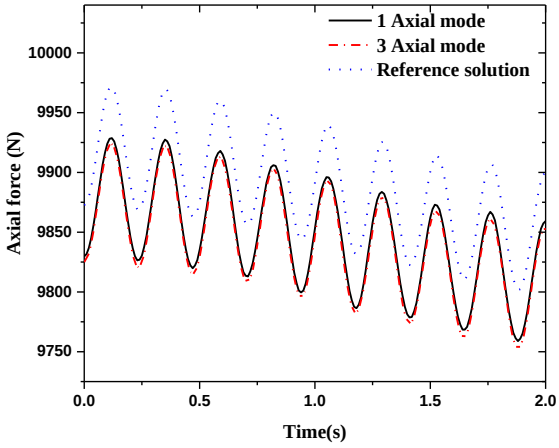

FIGURE 4: THE VARIATION OF THE AXIAL LOAD AT THE ENDPOINT VERSUS TIME

In Figures 4 and 5, the value of the axial forces at different time instants are depicted for the system that does not include axial modes and the system with one and three axial modes. Accordingly, it can be seen that by having axial modes, the value of axial load changes. Moreover, adding more axial load can also change the value of the axial load at the endpoint. However, as can be seen in Figure 2, these differences do not significantly change the final position of the payload. In Figure 4, it can clearly be seen that the value of the axial load for the cases including axial modes is lower than the case without axial mode. The main reason can be due to the fact that in the case without axial mode, the axial force is constant within the wire rope and equal to the mean value of the axial force at two ends of the wire ropes. However, for two other cases, this force is a trigonometric function changing within time along the wire rope. Hence, the integration of this constant value is a larger value than the non-constant trigonometric function.

Furthermore, in Figure 5, it can be observed that the difference between the case without axial mode and the case including one and three axial modes. Accordingly, the absolute value of this difference for the case with one axial mode is lower than the one with three axial modes. The reason for this difference can be explained by the deformed shape of the string where in the case with one mode, it is closer to the constant value of axial force compared to the case with three mode. As a result, the summation of this difference along the wire rope is lower.

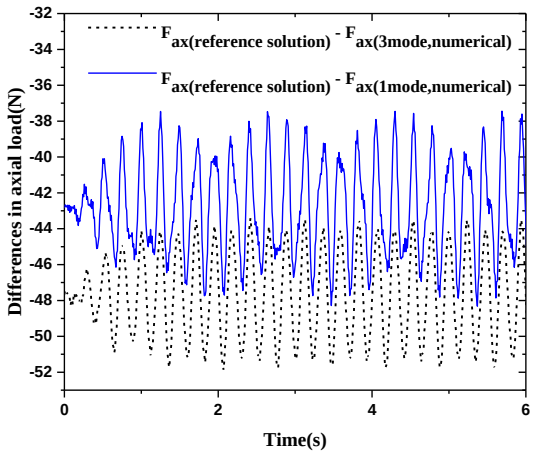

FIGURE 5: DIFFERENCES BETWEEN THE AXIAL FORCES AT THE END OF THE WIRE ROPE

5. CONCLUSION

This research has addressed the dynamic behavior of reeving systems by describing the axial deformation as a set of absolute nodal coordinates and modal coordinates. According to the results, it can be seen that by adding more modes, the variation of the axial load is not constant and approaches a more realistic state. Although the payload position does not significantly change, the value of the axial force undergoes changes.

ACKNOWLEDGEMENTS

This research was funded by European Union's Horizon 2020 research and innovation program under the Marie Skłodowska-Curie project No. 860124 (THREAD).

REFERENCES

[1] Escalona, J.L., 2017. "An arbitrary Lagrangian–Eulerian discretization method for modeling and simulation of reeving

systems in multibody dynamics". Mechanism and Machine Theory, 112, pp.1-21.

[2] Lugrís, U., Escalona, J.L., Dopico, D. and Cuadrado, J., 2011. "Efficient and accurate simulation of the rope–sheave interaction in weight-lifting machines". Proceedings of the Institution of Mechanical Engineers, Part K: Journal of Multi-body Dynamics, 225(4), pp.331-343.

[3] Escalona, J.L., Orzechowski, G. and Mikkola, A.M., 2018. "Flexible multibody modeling of reeving systems including transverse vibrations". Multibody System Dynamics, 44(2), pp.107-133.

[4] Lang, H. and Arnold, M., 2012. Numerical aspects in the dynamic simulation of geometrically exact rods. Applied Numerical Mathematics, 62(10), pp.1411-1427.

[5] Rouvinen, A., Lehtinen, T. and Korkealaakso, P., 2005. Container gantry crane simulator for operator training. Proceedings of the Institution of Mechanical Engineers, Part K: Journal of Multi-body Dynamics, 219(4), pp.325-336.

[6] Buckham, B.J. and Nahon, M., 2001. Formulation and validation of a lumped mass model for low-tension ROV tethers. International Journal of Offshore and Polar Engineering, 11(04)

[7] Godbole, H.A., Caverly, R.J. and Forbes, J.R., 2018. Modelling of flexible cable-driven parallel robots using a Rayleigh-Ritz approach. In Cable-driven parallel robots, pp. 3-14. Springer, Cham.

[8] Gerstmayr, J. and Irschik, H., 2008. On the correct representation of bending and axial deformation in the absolute nodal coordinate formulation with an elastic line approach. Journal of Sound and Vibration, 318(3), pp.461-487.

[9] Gerstmayr, J. and Shabana, A.A., 2006. Analysis of thin beams and cables using the absolute nodal co-ordinate formulation. Nonlinear Dynamics, 45(1), pp.109-130.

[10] Chen, K.D., Liu, J.P., Chen, J.Q., Zhong, X.Y., Mikkola, A., Lu, Q.H. and Ren, G.X., 2020. "Equivalence of Lagrange's equations for non-material volume and the principle of virtual work in ALE formulation". Acta Mechanica, 231(3), pp.1141-1157.

[11] Zhang, H., Guo, J.Q., Liu, J.P. and Ren, G.X., 2020. "An efficient multibody dynamic model of arresting cable systems based on ALE formulation". Mechanism and Machine Theory, 151, p.103892.

[12] Kaczmarczyk, S. and Ostachowicz, W., 2003. Transient vibration phenomena in deep mine hoisting cables. Part 1: Mathematical model. Journal of Sound and Vibration, 262(2), pp.219-244.

[13] Qi, X., Zhang, R. and He, Q., 2019, May. Modeling and Analysis of Transverse Vibration of Traction Rope of High Speed Traction Elevator. In IOP Conference Series: Materials Science and Engineering (Vol. 538, No. 1, p. 012036). IOP Publishing.

[14] Wang, L., Cao, G., Wang, N. and Zhang, Y., 2020. Dynamic Behavior Analysis of a High-Rise Traction System with Tensioned Pulley Acting on Compensating Rope. Symmetry, 12(1), p.129.

[15] Wang, J., Qi, Z. and Wang, G., 2017. Hybrid modeling for dynamic analysis of cable-pulley systems with time-varying length cable and its application. Journal of Sound and Vibration, 406, pp.277-294.